Bacteriophage T7 RNA polymerase and its active-site mutants. Kinetic, spectroscopic and calorimetric characterization

ARTICLE *in* JOURNAL OF MOLECULAR BIOLOGY · APRIL 1994

Impact Factor: 4.33 · DOI: 10.1006/jmbi.1994.1205 · Source: PubMed

J. Mol. Biol. (1994) **237**, 5–19

Bacteriophage T7 RNA Polymerase and Its Active-site Mutants

Kinetic, Spectroscopic and Calorimetric Characterization

Patricia A. Osumi-Davis[1], Narasimha Sreerama[1], David B. Volkin[2] C. Russell Middaugh[2], Robert W. Woody[1] and A-Young Moon Woody[1]†

[1]*Department of Biochemistry, Colorado State University Fort Collins, CO 80523, U.S.A.*

[2]*Department of Pharmaceutical Research, Merck Research Laboratories West Point, PA 19486, U.S.A.*

It has been demonstrated that the amino acids Asp537, Asp812, Lys631, His811 and Tyr639 are involved in bacteriophage T7 RNA polymerase catalysis. In the present paper, we report kinetic, spectroscopic and calorimetric characterization of the wild-type and mutant T7 RNA polymerases generated at these five loci (D537N, E; K631M, R; Y639F, S, A, W; H811Q, A; D812N, E). The wild-type enzyme has a substantial amount of secondary structure as determined by CD analysis (α-helix, 43%; β-sheet, 14%; β-turn, 25%; unordered, 18%). The CD spectra of 12 mutants at five loci are very similar to that of the wild-type, except for the mutant Y639W. Within experimental error, the thermal transition temperatures measured by CD and DSC as well as the λ_{max} values of the fluorescence spectra were the same for the wild-type and all of the mutants. Therefore, the overall folding and stability of the mutant enzymes are very similar to those of the wild-type enzyme, although small local conformational changes cannot be excluded. For the synthesis of the pentamer pppGGACU, the mutants D537E and D812E showed an approximately two- to threefold decrease in $(k_{cat})_{app}$ and an approximately two- to threefold increase in $(K_m)_{app}$, relative to the wild-type, in contrast to the mutants D537N and D812N which exhibited no detectable activity. The mutant K631R showed a sevenfold reduction in $(k_{cat})_{app}$ and a two- to threefold increase in $(K_m)_{app}$, supporting our earlier observation with the mutant K631M that Lys631 may be involved in phosphodiester bond formation. The mutant Y639S can synthesize the trimer GGA with an approximately 50-fold decrease in $(k_{cat})_{app}$ and a tenfold increase in $(K_m)_{app}$, relative to the wild-type, underlining the importance of the phenyl ring of Tyr639. The mutant H811A, in which the side-chain at position 811 is incapable of forming a hydrogen bond, can synthesize the trimer GGA with an approximately tenfold decrease in $(k_{cat})_{app}$ and an approximately 35-fold increase in $(K_m)_{app}$. Thus, either the hydrogen-bonding capacity of this residue is non-essential or some other group can functionally substitute for the His811 side-chain. The wild-type enzyme showed significant effects of the base position in the sequence on the apparent binding constants for the NTPs. The kinetics of GpG-primed trimer, tetramer and pentamer synthesis on three 22 bp templates were investigated for the wild-type and mutant enzymes with measurable activity. The rate of oligonucleotide synthesis depends strongly on the message sequence, and abortive termination occurs more frequently following UMP incorporation. For a given template, the rate of synthesis by the wild-type and all the mutants is trimer > pentamer (run-off transcript) > tetramer. The effect of the 5′-triphosphate in the initiating nucleotide is minimal for the wild-type and mutant enzymes. The apparent pK values obtained from the high-pH side of the pH-activity profiles of the wild-type and the mutants K631R and Y639F are the same within experimental error, implying that an amino acid(s) other than Lys631 or Tyr639 is responsible for the high-pH side of the pH-activity profile.

Keywords: T7 RNA polymerase; transcription; site-directed mutagenesis; differential scanning calorimetry; CD

† Author to whom all correspondence should be addressed.

0022-2836/94/110005-15 $08.00/0

1. Introduction

The transcription process, in which RNA is synthesized on a DNA template, is one of the most central in biology. In addition to the vital role of synthesizing RNA, transcription is subject to critical regulation. RNA polymerase is the central enzyme responsible for transcription. Bacteriophage T7 RNA polymerase, a single subunit enzyme (99 kDa), is one of the simplest known RNA polymerases, and can serve as a model for mechanistic studies on many aspects of transcription. Its gene has been cloned (Davanloo *et al.*, 1984; Tabor & Richardson, 1985) and therefore it can be produced in substantial quantities for biochemical and biophysical studies. To understand the mechanism of RNA synthesis, it is essential to determine the identity of catalytically significant residues, how they are arranged in the active site of the enzyme, and ultimately how these functional groups participate in the transcription process.

Five amino acid loci are conserved throughout a wide variety of DNA and RNA polymerases (Delarue *et al.*, 1990), and a sixth locus is conserved in viral and mitochondrial RNA polymerases and in bacterial DNA pol I sequences. In T7 RNA polymerase, the fully conserved residues are Asp537, Lys631, Tyr639, Gly640 and Asp812, while His811 is conserved over a narrower range of polymerases. We recently reported (Osumi-Davis *et al.*, 1992) the generation and initial biochemical characterization of five mutants in which each of the conserved loci with a functional side-chain had been mutated to an approximately isosteric amino acid residue (D537N, K631M, Y639F, H811Q, D812N). Residues Asp537 and Asp812 are essential and Lys631 and His811 are significantly involved in T7 RNA polymerase catalysis, while the hydroxyl group on the phenyl ring of Tyr639 may not contribute significantly to catalysis (Osumi-Davis *et al.*, 1992). We have proposed tentative roles for these five amino acids (Osumi-Davis *et al.*, 1992). The negatively charged carboxylates of Asp537 and/or Asp812 may participate in the abstraction of the 3′-OH proton of the growing RNA chain, or in a "charge relay" system with a His or other base which abstracts the proton from the 3′-OH of the growing chain, or in binding Mg^{2+} with which the incoming NTP is complexed. His811 could function to enhance the nucleophilicity of an Asp residue, in which case the His→Gln substitution would be expected to diminish but perhaps not eliminate the enhancement. Lys631 may help stabilize the transition state by ionic interactions, perhaps by binding one of the phosphoryl oxygens. The observed apparent pK ($\approx$9·5) for the high-pH side of the activity-pH profile of T7 RNA polymerase could be due to titration of a somewhat perturbed Lys. The phenolic-OH of Tyr639 seems to play an insignificant role, although the mutant Y639F gives somewhat altered kinetic parameters.

In order to further elucidate the roles of these amino acids, additional mutations were introduced at these amino acid loci to generate mutants (D537E, K631R, Y639A, Y639S, Y639W, H811A and D812E) which retain enough activity to permit further kinetic studies. Alterations in enzyme activity resulting from a mutation at a specific locus indicate either that the mutated locus is part of the active site or that the mutation has induced a conformational change which indirectly affects the active site. It is therefore essential to exclude conformational changes as rigorously as possible before a mutation which alters enzyme activity is interpreted as evidence that the mutated residue plays a role in the active site. In this paper, kinetic, spectroscopic and calorimetric data on the wild-type and the 12 mutants generated at these five loci will be presented, and the functional roles of these amino acids will be examined and discussed in light of our new data and the recently published crystal structure of the enzyme at 3·3 Å resolution (Sousa *et al.*, 1993).

2. Materials and Methods

(a) *Preparation of the wild-type and the mutant T7 RNA polymerases*

The methodology to produce mutants (using BioRad Muta-Gene Phagemid In Vitro Mutagenesis, Version 2) and the purification of the wild-type and mutant T7 RNA polymerases were the same as previously described (Osumi-Davis *et al.*, 1992).

The seven 21 to 24 nucleotide oligonucleotides used for mutagenesis are represented here by the base changes relative to the wild-type sequence: (D537E)(G→C); (K631R)(T→C); (Y639A)(T→G)(A→C); (Y639S)(T→G); (Y639W)(G→C)(G→C); (H811A)(T→G)(G→C); (D812E)(G→C).

These oligonucleotides were synthesized in the Macromolecular Resources Facility, Department of Biochemistry and Molecular Biology, Colorado State University, Fort Collins, CO 80523, U.S.A.

(b) *Transcription assay and steady-state kinetics*

The procedures for transcription assay and steady-state kinetics have been described (Osumi-Davis *et al.*, 1992). Briefly, the transcription reactions were carried out at 37°C for 5 min in 50 mM-Tris·HCl (pH 7·9), 1 mM-dithiothreitol (DTT) and 10 mM-$MgCl_2$ for DE81 filter-binding in order to compare with our earlier values. All other transcription reactions were carried out in 40 mM-Tris·HCl (pH 7·9), 10 mM-$MgCl_2$, 10 mM-KCl, 1 mM-DTT, 0·1 mM-EDTA, with 20 to 200 nM-enzyme, (α-^{32}P)-labeled-nucleotide, variable or saturating concentrations of nucleotides (see Figure legends for the relevant details) and 100 to 200 nM template. The templates used were pT713 plasmid DNA containing the T7 class III promoter, either supercoiled or linearized with *Bam*HI, or 22 bp oligonucleotide templates. The 22 bp oligonucleotide templates were (the +1 residue is indicated by italics): template A, 5′-TAATACGACTCACTATA*GG*ACT-3′; template U, 5′-TAATACGACTCACTATA*GG*TAC-3′; template C, 5′-TAATACGACTCACTATA*GG*CTA-3′.

The reaction products were analyzed either by DE81 filter-binding assay (Reisbig *et al.*, 1979) or by urea/25% polyacrylamide gel electrophoresis (PAGE), and quantitated using a PhosphorImager SP (Molecular Dynamics,

Sunnyvale, CA). Analysis of RNA products by the PhosphorImager technique allowed quantitation of the bands with a high degree of accuracy and sensitivity. For the wild-type and mutant T7 RNA polymerases which retain enzyme activity, time-dependent RNA synthesis was monitored to assure that the initial slope was linear within the time of measurement. The steady-state kinetics data (NTP binding) for the synthesis of pppGGACU were subjected to Wilkinson's (1961) statistical analysis to obtain $(K_m)_{app}$ and $(k_{cat})_{app}$ values and standard errors, after graphs were drawn as Hanes' plots (substrate/velocity *versus* substrate). For promoter binding, data were fit to the kinetic equation (eqn (2) of Martin & Coleman, 1987) using the Levenberg–Marquardt algorithm for non-linear least-squares (Press *et al.*, 1989). The $(k_{cat})_{app}$ values for the pentamers, tetramers and trimers, synthesized in the presence of a dinucleotide initiator GpG, were calculated from the enzyme activity data obtained under saturating nucleotide and promoter concentrations (see Figure legends for details).

(c) *Absorption and CD measurements*

The concentration of T7 RNA polymerase was determined from the absorbance at 280 nm measured on a Cary 118C spectrophotometer using an extinction coefficient of $1{\cdot}4 \times 10^5\ M^{-1}\ cm^{-1}$ (King *et al.*, 1986). The same extinction coefficient was used for the mutants, including the Y639 mutants, because these values will differ from that of the wild-type by at most 1%.

The CD spectra of the wild-type and mutant T7 RNA polymerases were measured in the range 180 to 260 nm with a JASCO model J720 spectropolarimeter at a scan rate of 100 nm min^{-1} and 0·1 nm resolution. The pathlengths of the cells used were 0·05 to 0·1 cm. Most spectra were recorded as an average of 10 scans. Appropriate buffer baseline spectra were subtracted from the protein spectra. Mean residue ellipticity was calculated using a mean residue weight of 112. The buffers used were 20 mM phosphate buffer (pH 7·8) and 6 mM phosphate buffer (pH 7·2), 120 mM NaCl.

(d) *Secondary structure analysis*

The observed CD spectra were analyzed for secondary structure content using the self-consistent method (Sreerama & Woody, 1993). Uncertainties in the secondary structure content can be estimated from the r.m.s. deviations obtained when proteins of known structure are analyzed. r.m.s. deviations of ±0·09, ±0·08, ±0·04, ±0·06 have been reported for the fractions of α-helix, β-sheet, β-turn and unordered structures, respectively (Sreerama & Woody, 1993). The CD spectra of the basis proteins were kindly provided by Dr W. C. Johnson, Jr. The fractions of the protein secondary structures were taken from Kabsch & Sander (1983), based on the analysis of X-ray structure. CD spectra in the range 185 to 260 nm were used in the analysis because of the poor signal/noise ratio below 185 nm.

(e) *Fluorescence spectra*

Fluorescence spectra were obtained with an SLM 8000 spectrofluorometer. Protein samples were dialyzed at 4°C against 6 mM phosphate buffer (pH 7·2), 120 mM NaCl. Following dialysis, the protein sample was diluted to 0·1 mg ml^{-1} with the same buffer. Samples were placed in a 2 mm × 1 mm quartz cuvette and fluorescence spectra were collected between 310 and 450 nm at 10°C employing excitation at 295 nm and a 1 nm bandpass.

(f) *Differential scanning calorimetry*

Calorimetry experiments were performed with a Hart 7708 calorimeter at a scan speed of 60°C h^{-1}. Protein samples were dialyzed as described above and diluted to a final concentration of 1 mg ml^{-1} protein. Sample volume was 0·6 ml and small sections of glass tubing were added to the sample to minimize interference from exotherms due to aggregation (Steadman *et al.*, 1988). Thermograms were corrected for background. All thermal transitions were irreversible, as judged by rescanning.

3. Results

(a) *Transcriptional characteristics of the wild-type and the mutant T7 RNA polymerases*

The amino acid sequence of T7 RNA polymerase (Moffatt *et al.*, 1984) containing the proposed catalytically significant amino acids (Osumi-Davis *et al.*, 1992) and the regions labeled (Knoll *et al.*, 1992) by a nucleotide photoaffinity analog, 8-azidoATP, are shown in Figure 1. The five amino acid loci mutated to generate the 12 site-directed mutants (D537N, E; K631M, R; Y639F, S, W, A; H811Q, A; D812N, E) are highlighted. The overall activities of the wild-type and the 12 mutant enzymes determined on pT713-supercoiled and *Bam*HI-linearized plasmid templates containing the T7 class III promoter are shown in Table 1. It is apparent that the overall activity has been reduced from $\sim 10^{+5}$ units for the wild-type enzyme to zero for some mutants and by one or more orders of magnitude for most other

Table 1
Enzyme activity of the wild-type and mutant T7 RNA polymerases

Enzyme	Activity†	Activity‡
WT	$3{\cdot}4 \times 10^5$	$1{\cdot}6 \times 10^4$
D537N		
D537E	$8{\cdot}3 \times 10^4$	$3{\cdot}1 \times 10^3$
K631M	$2{\cdot}0 \times 10^4$	$3{\cdot}2 \times 10^2$
K631R	$4{\cdot}9 \times 10^4$	$1{\cdot}7 \times 10^3$
Y639F	$2{\cdot}5 \times 10^5$	$1{\cdot}8 \times 10^4$
Y639A		
Y639S	$1{\cdot}1 \times 10^3$	$2{\cdot}1 \times 10^2$
Y639W		
H811A		
H811Q	$6{\cdot}5 \times 10^4$	$4{\cdot}5 \times 10^3$
D812N		
D812E	$1{\cdot}1 \times 10^5$	$2{\cdot}9 \times 10^3$

The enzyme activity (in units) of the wild-type (WT) and mutant RNA polymerases was determined in a 50 μl reaction mixture containing 50 mM Tris·HCl (pH 7·9), 10 mM $MgCl_2$, 1 mM DTT, 50 nM T7 RNA polymerase, 200 nM pT713 template, 3 mM GTP, 400 μM ATP and CTP and 800 μM UTP, and analyzed by DE81 filter-binding assay (Reisbig *et al.*, 1979). One unit of specific activity is defined as 1 nmol of UMP incorporation per mg of enzyme per h at 37°C under our assay conditions.

† Template was pT713 supercoiled plasmid.

‡ Template was pT713-*Bam*H1-linearized plasmid.

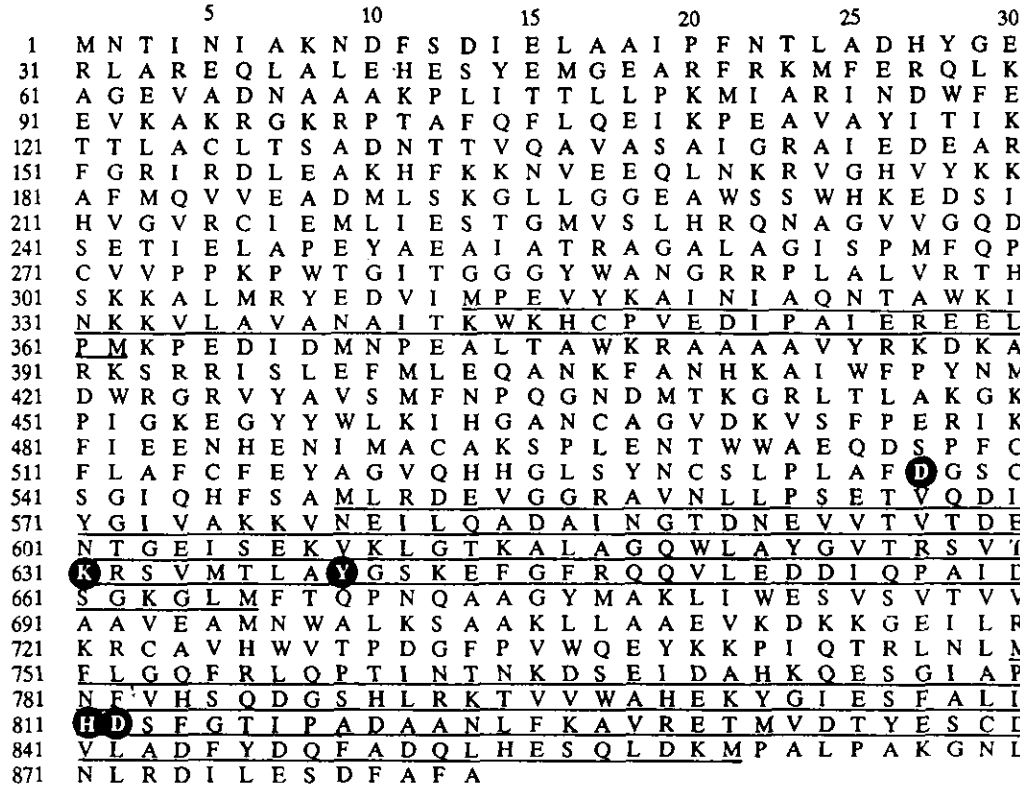

Figure 1. T7 RNA polymerase amino acid sequence (Moffatt *et al.*, 1984). The underlined regions (P314 to M362, L550 to M666, and F751 to M861) are the peptide regions photolabeled with 8-azidoATP (see Knoll *et al.*, 1992) and the bold black circled amino acids are the functional amino acids conserved in RNA and DNA polymerases (Delarue *et al.*, 1990).

mutants. These results are consistent with the catalytic significance of these loci. The wild-type and mutant T7 RNA polymerases were purified to greater than 95% homogeneity by identical purification procedures. This suggests that there is no gross conformational change in the mutants which is reflected in their chromatographically sensitive surface properties. In addition, their structural integrity was examined and their overall protein folding was found to be similar to that of the wild-type enzyme as described in the next section.

To obtain better defined transcriptional activities of these mutants, 60 nt run-off transcripts were synthesized by the wild-type and the mutant enzymes on pT713-*Bam*HI linearized plasmid template with saturating concentrations of the nucleotides (4 mM GTP, 400 μM ATP and CTP and 800 μM UTP) and were analyzed by urea/25% PAGE and quantitated. The results are shown in Figure 2. The mutants D537E and D812E have, respectively, ~20% and ~15% of the wild-type activity for the synthesis of the 60 nt run-off transcript, in contrast to the mutants D537N and D812N, which had no detectable activity. These results reinforce our previous observation that a negative charge or the ability to accept a proton is essential at positions 537 and 812. The mutants Y639S, Y639A and Y639W have no detectable activity for producing the 60 nt run-off transcript. It has been shown that the mutant Y639F, which has the phenyl ring but no OH-group, retains enzymatic activity for 60 nt RNA synthesis comparable to or slightly higher than that of the wild-type enzyme. These results highlight the necessity of the phenyl ring at this position for T7 RNA polymerase activity. Since the mutant Y639W showed an anomalous band in the mobility shift assay for the enzyme–DNA interaction in addition to the expected band (data not shown), and a reduced CD amplitude (see next section) suggesting a perturbed conformation, we did not characterize this mutant further. The mutant H811A showed no activity for the synthesis of 60 nt RNA, as opposed to 30% activity for the mutant H811Q, which has glutamine in place of histidine and is, therefore, capable of forming a hydrogen bond. However, the mutant H811A retains some 3 to 10% and 20 to 30% activity, respectively, for synthesis of pentamers and trimers. Further studies are necessary to explain why this mutant with Ala at position 811, which is incapable of forming a hydrogen bond, can still synthesize short oligonucleotides. The mutant K631R which retains a positive charge at position 631 has 10% of the wild-type activity for the synthesis of the 60 nt RNA. This contrasts with the results for the mutant K631M, which has no detectable activity for the synthesis of the 60 nt RNA.

Even under conditions of saturating nucleotides, the wild-type T7 RNA polymerase produced abortive initiation products in addition to the 60 nt

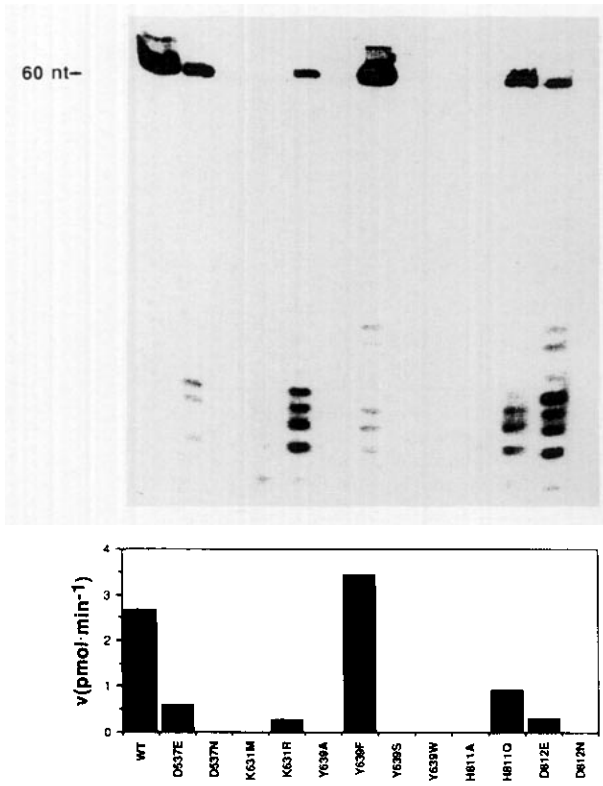

Figure 2. Autoradiogram and histogram of run-off transcription products catalyzed by the wild-type and the mutant T7 RNA polymerases under saturating nucleotide concentrations. The transcripts were synthesized on 100 nM pT713-*Bam*HI-linearized plasmid DNA (see Materials and Methods for details) in 40 mM Tris·HCl (pH 7·9), 10 mM $MgCl_2$, 10 mM KCl, 1 mM DTT, 0·1 mM EDTA with 20 nM enzyme, 5 μCi [α-^{32}P]UTP, 4 mM GTP, 400 μM ATP, CTP and UTP at 37 °C for 5 min.

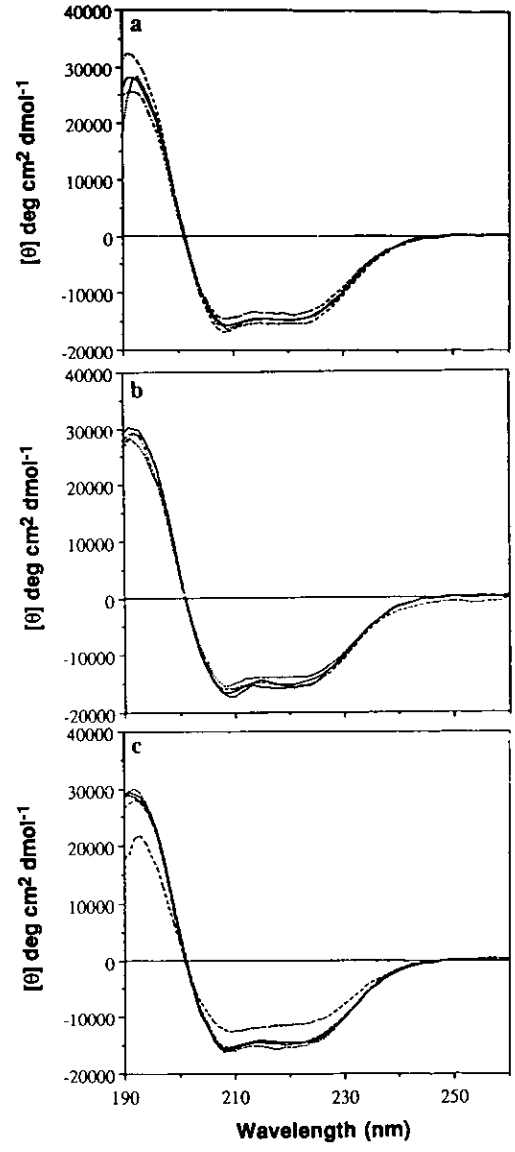

Figure 3. CD spectra of the wild-type and mutant T7 RNA polymerases in 20 mM phosphate buffer (pH 7·8). (a), Wild-type (——); D537E (····); K631M (– – – –); K631R (—·—·—·). (b), D812E (– – – –); Y639F (····); Y639S (—·—·—·); H811Q (– – – –). (c), D537N (——); Y639A (····); Y639W (– – – –); H811A (—·—·—·); D812N (– – – –). Each spectrum is an average of 2 to 3 independently obtained spectra and the error is about ±5%.

RNA (Figure 2). This is in accordance with the previous observation (Martin *et al.*, 1988) that abortive initiation is a part of normal transcription catalyzed by T7 RNA polymerase. The mutant T7 RNA polymerases, except for Y639F, exhibited a higher ratio of abortive (3 to 15 nt) products to the 60 nt transcripts than the wild-type enzyme (Figure 2 and Table 2).

(b) *Secondary structures of the wild-type and mutant T7 RNA polymerases analyzed by CD*

Since CD spectroscopy is very sensitive to the conformation and structure of biopolymers, we have applied this technique to the wild-type and mutant T7 RNA polymerases in 20 mM phosphate buffer (pH 7·8) (Figure 3). The results of a secondary structure analysis of these CD spectra are given in Table 3. The α-helix, β-sheet, β-turn and unordered structural contents of the wild-type T7 RNA polymerase are 43, 14, 25 and 18%, respectively. No appreciable changes in the secondary structural contents were detected in 6 mM phosphate buffer (pH 7·2), 120 mM NaCl or 1 mM EPPS† buffer (pH 7·8), 50 mM KCl. With the exception of the mutant Y639W, which has a somewhat reduced α-helix content, the secondary structural composition of the mutants cannot be distinguished from that of the wild-type enzyme within the experimental error (Table 3) despite the dramatic differences in enzyme activity seen among the various proteins. As was noted previously (Osumi-Davies *et*

† Abbreviations used: EPPS, *N*-(2-hydroxyethyl)-piperazine-*N*′-3-propanesulfonic acid; DSC, differential scanning calorimetry; WT, wild-type.

Table 2
Relative transcript production

Enzyme	60 nt RT†	60 nt RT‡	AbT§	60 nt RT‡ Total‖	AbT Total
WT	100	6·70±0·67	1·47	0·85	0·15
D5267E	20	1·48±0·15	1·55	0·49	0·51
K631M¶	—	—	0·45	—	1·0
K631R	8±3	0·70±0·20	3·38	0·17	0·83
Y639F	129±23	8·60±2·50	1·75	0·83	0·17
H811A¶	—	—	0·23	—	1·00
H811Q	30±5	2·33±0·40	2·15	0·52	0·48
D812E	14±6	0·73±0·30	4·63	0·14	0·86

Transcription assays were performed on pT713-*Bam*HI-linearized plasmid template and quantitated as described in Materials and Methods. Mutants discussed in this paper but not appearing in the Table have activities too low for reliable quantitation. Reaction solution contained 200 nM pT713-*Bam*HI, 20 nM enzyme, 4 mM GTP, 400 μM ATP, 5 μCi [α-^{32}P]ATP (3000 Ci/mmol), 400 μM CTP and 800 μM UTP. These are averages of 2 to 3 independent experiments.

† 60 nt run-off transcript expressed as % wild-type activity.

‡ 60 nt run-off transcript expressed as velocity (min^{-1}).

§ Abortive transcript, 3 to 15 nt in length, expressed as velocity (min^{-1}).

‖ 60 nt RT (‡) plus AbT (§).

¶ These mutants did not produce measurable amounts of run-off transcript but abortive transcript and/or trimer (pentamer) transcripts could be quantitated.

al., 1992), we cannot exclude the possibility that local conformational changes not detected by CD and fluorescence measurements (see below) might have an effect on the enzymatic activity, but the data shown in this paper clearly exclude substantial conformational alterations induced by the mutations under study.

(c) *Overall conformation and thermal transitions monitored by CD, DSC and fluorescence*

Thermal melting transitions of the wild-type and mutant enzymes have been measured by CD and DSC in 6 mM phosphate buffer (pH 7·2), 120 mM NaCl. The T_m values obtained by the two methods agreed well and showed no more than 2 °C variation from that of the wild-type (47(±2)°C) for any of the mutants. These results are given in the third and fourth columns of Table 4. Figure 4 displays typical DSC curves of the wild-type T7 and several mutant RNA polymerases. A major unfolding event is observed at ~47 °C for all of the enzymes. Small pretransitions were occasionally seen at ~35 °C but were not consistently reproducible, while interference from protein aggregation was observed at temperatures above 60 °C. Nevertheless, the breadth and lack of symmetry of the endotherms suggest that the proteins are not undergoing simple co-operative unfolding transitions.

Fluorescence spectroscopy was also utilized to analyze the conformation of the wild-type and mutant enzymes. The λ_{max} for emission (339 nm) was identical within 1 nm for all of the enzymes (Table 4). Although there is only one Trp in the N-terminal 20% of the sequence, there are 18 Trp residues distributed rather evenly throughout the

Table 3
Secondary structure of the wild-type and the mutant T7 RNA polymerases

Enzyme	*T* (°C)	Helix	Sheet	Turns	Unordered
WT	25	0·43	0·14	0·25	0·19
	37	0·41	0·15	0·25	0·19
	50	0·30	0·22	0·14	0·35
D537N	25	0·44	0·14	0·25	0·19
D537E	25	0·43	0·13	0·29	0·15
K631M	25	0·43	0·15	0·23	0·21
K631R	25	0·40	0·16	0·26	0·18
Y639F	25	0·40	0·16	0·26	0·20
Y639A	25	0·42	0·14	0·24	0·21
Y639S	25	0·40	0·13	0·25	0·21
Y639W	25	0·37	0·13	0·27	0·22
H811Q	25	0·43	0·15	0·24	0·21
H811A	25	0·40	0·15	0·26	0·20
D812N	25	0·44	0·11	0·28	0·19
D812E	25	0·43	0·15	0·23	0·21

Secondary structures are given as fractions. Secondary structural analysis was performed on each of 2 or 3 experimental spectra obtained for each protein and the average values are reported. The error is about ±5%.

Table 4
Melting temperature and fluorescence emission maximum of the wild-type and mutant T7 RNA polymerases

Enzyme	λ_{max} (nm)	T_m (°C) CD	T_m (°C) DSC
WT	339	47±2	49±1
D537N	339	50±2	50±1
D537E	339	47±2	49±1
D812N	338	48±2	49±1
D812E	338	48±2	49±1
K631M	339	50±2	49±1
Y639F	339	49±2	49±1
Y639A	339	48±2	49±1
Y639S	338	47±2	49±1
H811Q	339	49±2	48±1
H811A	338	48±2	49±1

C-terminal 80%. Though it is uncertain how many of these contribute significantly to the fluorescence spectrum, the absence of any detectable perturbation of the emission maximum by the mutations studied here indicates that few, if any, of the emitting Trp residues experience significant changes in their environment. This is consistent with the conclusions from CD and DSC that any conformational changes induced by the mutations under study must be local in character.

(d) *Steady-state kinetic parameters of the wild-type and mutant T7 RNA polymerases for the synthesis of pppGGACU on a 22 bp template*

The ability of the mutant T7 RNA polymerases to bind DNA and nucleotides and to form phosphodiester bonds was determined kinetically by examining the synthesis of pppGGACU on a 22 bp template (template A), which has a class III T7 promoter and the message sequence GGACT. This template allows the synthesis of a message including all four nucleotides. Steady-state kinetic parameters $(K_m)_{app}$ and $(k_{cat})_{app}$ thus obtained for the new mutants are compared with those for the previously described mutants in Table 5. Among the mutants

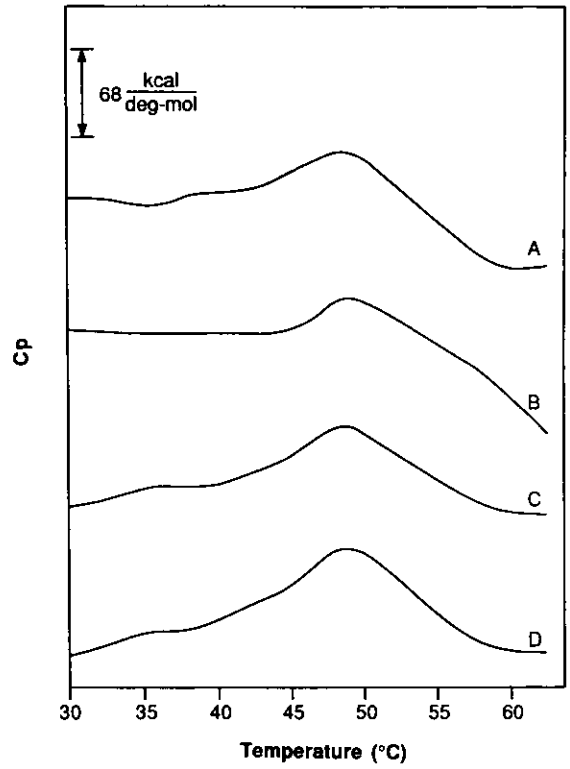

Figure 4. Thermal unfolding of the wild-type and mutant RNA polymerases as determined by DSC. A, Wild-type; B, Y639A; C, D812N; D, H811Q. Samples contained 1 mg/mgml^{-1} protein in 6 mM phosphate buffer (pH 7·2), 120 mM NaCl.

Table 5
Kinetic parameters for the synthesis of pppGGACU

	Kinetic parameters					
	$(K_m)_{app}$ (μM)					
Enzyme	GTP	ATP	CTP	UTP	Promoter	$(k_{cat})_{app}$ (min^{-1})
Wild-type†	366±43	13±2	10±1	100±11	0·013±0·005	28±6
D537E	430±230	14±2	7±1	128±27	0·030±0·002	13±6
K631M†		39±7	31±6	98±26		0·20±0·1
K631R	1467±400	15±5	46±4	318±40	0·006±0·002	4±0·4
Y639F†	1055±57	22±2	30±2	119±10	0·023±0·016	37±7
H811Q†	710±221	43±4	53±15	132±29	0·038±0·032	7±4
D812E	1388±530	22±4	22±2	350±142	0·017±0·005	11±5

Transcription assays and calculations of $(K_m)_{app}$ and $(k_{cat})_{app}$ were made as described in Materials and Methods. Nucleotide and promoter concentrations were kept at saturating levels (2 mM GTP; 0·8 mM ATP, CTP and UTP; 200 nM template A) except for varying nucleotide and promoter concentrations (5 to 100 μM ATP and CTP; 50 to 1000 μM UTP; 200 to 3000 μM GTP). For mutants discussed in this paper but not appearing in the Table, the activity for pentamer synthesis was too low to permit accurate determination of kinetic parameters.

† These values have been presented (Osumi-Davis *et al.*, 1992) but are shown here for comparison with the newly generated mutants. The $(k_{cat})_{app}$ values are half of the previous values due to an error in the enzyme concentration previously used for these enzymes. The overall conclusion of this previous work has not been affected by this error.

(D537E, K631M, K631R, Y639F, H811Q and D812E), K631M and K631R showed large reductions in $(k_{cat})_{app}$ (100-fold and 7-fold, respectively) in contrast to a few-fold increase in $(K_m)_{app}$. This supports the proposal that the mutations at position 631 have a major effect on phosphodiester bond formation. The rest of the mutants showed an approximately three- to fourfold decrease in $(k_{cat})_{app}$ and an approximately two- to fourfold increase in $(K_m)_{app}$. Although $(k_{cat})_{app}$ and $(K_m)_{app}$ are complex quantities, and their values should be interpreted with proper caution, as a first approximation it may be assumed that both nucleotide binding and phosphodiester bond formation are perturbed by mutations of Asp537, Tyr639, His811 and Asp812.

The $(K_m)_{app}$ values for the promoter interaction for the mutants are similar to that of the wild-type within experimental error. Those mutants which do not retain enough enzymatic activity to allow determination of kinetic parameters were examined by the electrophoretic mobility-shift assay (Osumi-Davis *et al.*, 1992). Within experimental error, there was no discernible difference between the wild-type and mutants, except for Y639W which manifested an additional band at the well (data not shown).

(e) *Nucleotide position-dependent* $(K_m)_{app}$ *values*

Our previous data (Osumi-Davies *et al.*, 1992) showed that the wild-type and mutant enzymes with measurable activity for the synthesis of the pentamer pppGGACU had the same $(K_m)_{app}$ for UTP, within experimental error, while the value of the $(K_m)_{app}$ was considerablty larger than the values obtained for the internal nucleotides A and C. The run-off transcript (5 nt) had UTP as the terminal nucleotide. Therefore, the question arose whether this was a specific effect of UTP or a positional phenomenon. We have therefore investigated the positional effect of the nucleotides on $(K_m)_{app}$ values for ATP, UTP and CTP using the wild-type enzyme and three different 22 bp oligonucleotide templates with varying message sequences (templates A, U and C). The results are summarized in Table 6. The $(K_m)_{app}$ values for ATP and UTP were the same for a given position, with the smallest value seen in the third position, and the values sequentially increasing in the fourth and fifth. By contrast, the $(K_m)_{app}$ values for CTP did not vary with position. Our results indicate that the relatively large $(K_m)_{app}$ values observed for UTP incorporation was not specific to UTP, but rather its position at the end of the message sequence, and the apparently invariant $(K_m)_{app}$(UTP) value for template A ($\sim 100\ \mu M$) observed for the wild-type and the mutants K631M, Y639F, H811Q (Osumi-Davies *et al.*, 1992) did not hold for the mutants, D812E and K631R (Table 5) which were found to be $350\ \mu M$ and $318\ \mu M$, respectively.

Table 6
Positional effect on nucleotide $(K_m)_{app}$ *values*

Pentamer sequence	$(K_m)_{app}$ (μM)		
pppGGACU	ATP 13±2	CTP 10±1	UTP 100±11
pppGGUAC	UTP 12±4	ATP 43±13	CTP 11±4
pppGGCUA	CTP 10±8	UTP 43±15	ATP 118±8

See Materials and Methods and Osumi-Davies *et al.* (1992) for experimental details and calculations of $(K_m)_{app}$. Three different pentamers were synthesized using templates A, U and C. Varying nucleotide concentrations ranged from 5 to 400 μM.

(f) *Synthesis of trimers, tetramers and pentamers on 22 bp templates*

In order to examine each step of nucleotide addition and the rate of dissociation of the product at a given step, we have synthesized trimer GGA, tetramer GGAC, and pentamer GGACU on template A in the presence of a dinucleotide initiator, GpG (Figure 5). The effect of nucleotide

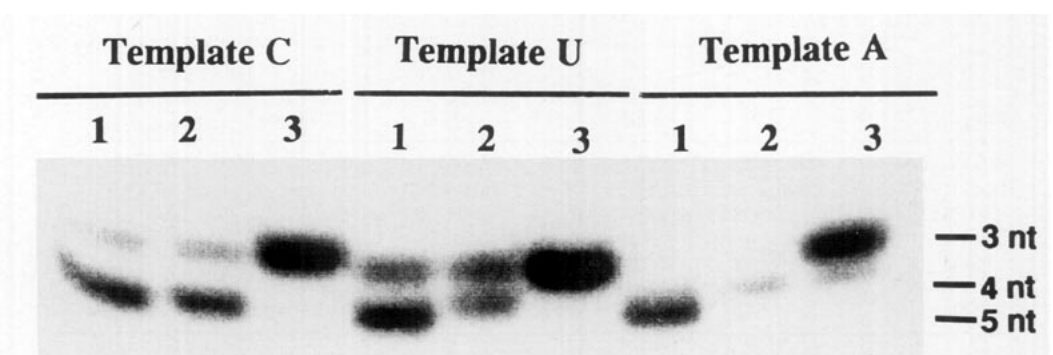

Figure 5. Autoradiogram of the pentamer, tetramer and trimer transcription products synthesized on templates A, U and C. Template C, 5 min reactions were carried out as described in Materials and Methods using 20 nM wild-type enzyme, 200 nM template C, 1 mM GpG, 5 μCi [α-^{32}P]CTP and the following nucleotides: 1, 400 μM CTP, UTP and ATP; 2, 400 μM CTP and UTP; and 3, 400 μM CTP. Template U, reactions are the same as for template C, except that template U; 5 μCi [α-^{32}P]UTP; and the following nucleotides; 1, 400 μM UTP, ATP and CTP; 2, 400 μM UTP and ATP; and 3, 400 μM UTP were used. Template A, reactions are the same as for template C, except that template A; 5 μCi [α-^{32}P]ATP; and the following nucleotides: 1, 400 μM ATP, CTP and UTP; 2, 400 μM ATP and CTP; and 3, 400 μM ATP were used.

Table 7

$(k_{cat})_{app}$ values (min^{-1}) for the synthesis of trimers, tetramers and pentamers

RNA / Enzyme	GGA	GGAC		GGACU	
		T†	B†	T†	B†
WT	15·0±2·0	0·3±0·1	1·3±0·5	0·1±0·1	11·0±1·0
D537E	8·0±3·0	0·3±0·2	0·6±0·1	0·1±0·1	2·9±1·0
K631M	0·2±0·1	0·1±0·1	0·1±0·1	0·1±0·1	—
K631R	8·3±3·2	0·2±0·1	0·8±0·2	0·1±0·1	1·4±0·2
Y639F	5·4±2·0	0·2±0·1	0·5±0·5	0·1±0·1	5·0±1·2
Y639S	0·2±0·1	—	0·1±0·1	—	—
H811A	4·2±1·0	0·3±0·1	0·9±0·3	0·3±0·1	0·5±0·3
H811Q	8·1±3	0·2±0·1	1·5±0·7	0·2±0·1	2·1±0·5
D812E	15·2±2·0	0·3±0·1	1·2±0·5	0·4±0·1	2·2±0·3
RNA / Enzyme	GGU	GGUA		GGUAC	
		T†	B†	T†	B†
WT	32·5±5·6	1·1±0·4	2·2±0·4	3·3±0·3	13·0±0·8
D537E	27·5±2·5	5·1±2·2	1·2±0·1	8·7±0·6	4·1±0·2
K631M	—	0·1±0·1	—	0·1±0·1	—
K631R	13·9±1·5	6·0±4·2	1·1±0·4	13·0±1·5	1·3±0·3
Y639F	12·7±2·3	0·5±0·3	0·8±0·2	1·8±0·2	6·2±0·1
Y639S	—	0·2±0·1		0·3±0·1	—
H811A	3·2±0·3	1·6±0·4	0·3±0·1	5·9±0·4	1·2±0·1
H811Q	6·0±0·1	2·3±1·2	0·6±0·1	4·1±1·2	2·0±0·1
D812E	41·8±3·00	7·50±1·3	3·5±0·1	22·6±0·5	4·1±0·2
RNA / Enzyme	GGC	GGCU		GGCUA	
		T†	B†	T†	B†
WT	20·0±5·8	1·2±0·1	5·7±0·7	1·0±0·1	6·3±0·2
D537E	5·3±0·1	1·2±0·1	1·5±0·2	1·3±0·1	1·9±0·3
K631M	0·2±0·1	0·8±0·1		0·5±0·1	—
K631R	7·3±0·5	3·5±0·4	1·4±0·1	2·7±0·2	1·2±0·1
Y639F	5·2±0·1	0·3±0·3	2·3±0·2	0·2±0·1	2·1±0·1
Y639S	0·3±0·1	0·6±0·1	—	0·1±0·1	0·1±0·1
H811A	4·4±0·5	2·9±0·3	0·4±0·1	2·9±0·2	0·7±0·2
H811Q	5·0±0·5	4·3±0·4	2·7±0·3	2·7±0·2	2·0±0·3
D812E	16·1±2·5	5·1±0·3	5·4±0·2	5·5±1·5	6·4±2·0

These are the $(k_{cat})_{app}$ values quantitated from experimental data analogous to the data shown in Figure 6 by means of PhosphorImager SP. See Materials and Methods and legend to Figure 5 for experimental details. RNA oligomers GGA, GGAC and GGACU are synthesized on template A; GGU, GGUA and GGUAC are synthesized on template U; GGC, GGCU and GGCUA are synthesized on template C.

† T stands for the top band (3 nt) and B stands for the bottom band (4 nt or 4 nt + 5 nt) in Figure 6.

position on transcription patterns was investigated by synthesizing GGU, GGUA, GGUAC, GGC, GGCU and GGCUA on two other templates, template U and template C. The RNA was labeled at the third nucleotide to follow the intermediate products also. The results show that synthesis of tetramers and pentamers produced not only the expected products but also trimers, and possibly tetramers in the case of pentamer synthesis. The pattern of the products varied with different templates, implying specific effects of the particular nucleotide sequence. We have also labeled the RNAs at the last nucleotide to visualize trimers, tetramers and pentamers alone. The numerical results of trimer, tetramer and pentamer synthesis are consistent with the values obtained previously by labeling the RNAs at the third position. Similar experiments were performed with each of the catalytically viable mutants, and the results are shown in Figure 6 and Table 7. The advantage of using the dinucleotide initiator GpG is that the product trimers were well-resolved from the tetramers and pentamers by urea/25% PAGE allowing quantitation of each band as shown in Figures 5 and 6. The migration velocities of the GpG-initiated trimers, tetramers and pentamers were found to be in the order: pentamers > tetramers > trimers. In addition, tetramers and pentamers synthesized on templates A and U manifested different mobilities. No such differences were seen on template C, however. Nevertheless, independent quantitation of tetramer and pentamer was not generally possible, either because of inadequate resolution or because the amount of tetramer produced was small in comparison with the pentamer. Since GpG lacks 5′-triphosphate, the apparent rate constants for the wild-type and mutants with viable activity were measured for the synthesis of GpG-initiated and GTP-initiated pentamers on template A and compared in Table 8. Likewise, the kinetic parameters for the synthesis of GpG-initiated and GTP-initiated trimers and tetramers by the wild-

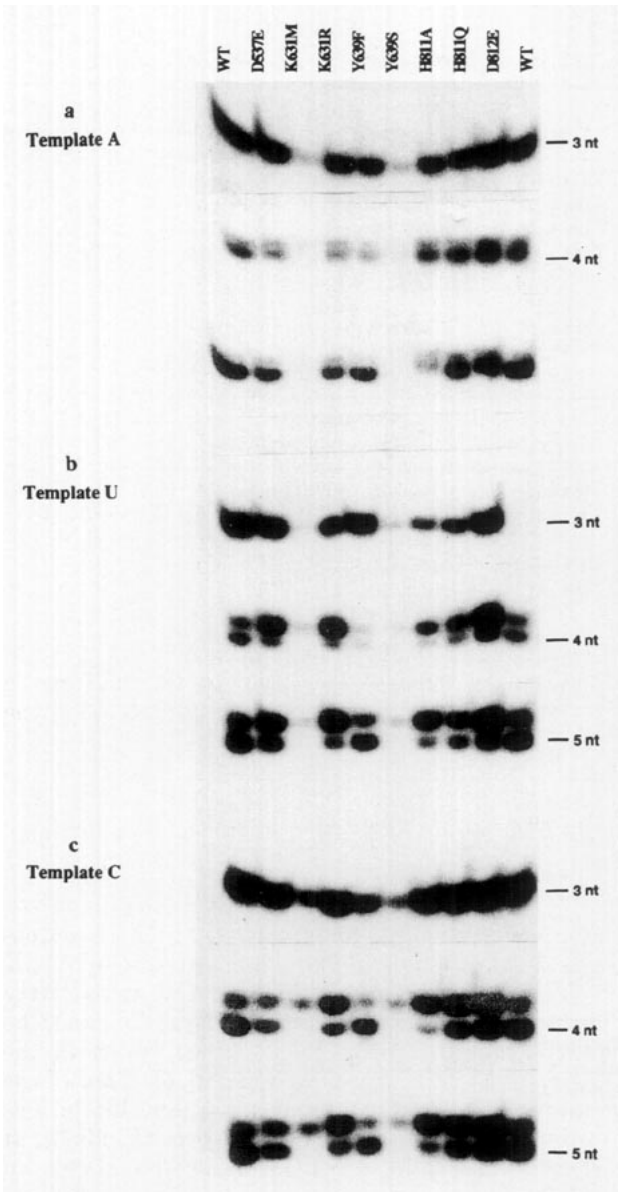

Figure 6. Autoradiograms of the trimers, tetramers and pentamers synthesized on templates A, U and C by the wild-type and mutant T7 RNA polymerases. Transcription products synthesized on template A (a), template U (b) and template C (c). Reaction conditions were the same as for the same template in Figure 5.

type enzyme were examined and are reported in Table 9. Although the actual values are somewhat variable, the rates of synthesis for the GpG-initiated and GTP-initiated oligonucleotides are comparable within a factor of 2. Even the rates of synthesis of the GTP-initiated pentamers measured by two different methods for a given enzyme only vary within this range (see Discussion). The $(K_m)_{app}$ values for ATP, CTP and UTP binding for GGACU and pppGGACU synthesis are not significantly different. Therefore, the effect of the 5′-triphosphate in the initiating nucleotide for oligonucleotide synthesis can be considered minimal.

It can be seen that the wild-type and catalytically active mutants, except perhaps for the Y639F,

Table 8

$(k_{cat})_{app}$ (min^{-1}) values for the synthesis of GpG-initiated and GTP-initiated pentamer synthesis on template A by the wild-type and mutant T7 RNA polymerases

Enzyme	GGACU†	pppGGACU‡	pppGGACU§
WT	11·0±1·0	19·0±2·0	28±6
D537E	2·9±1·0	4·6±1·0	13±6
K631M	—	0·4±0·1	0·2±0·1
K631R	1·4±0·2	1·2±0·2	4·0±0·4
Y639F	5·0±1·2	15·0±4·7	37±7
H811Q	2·1±0·5	2·7±0·3	7±4
D812E	2·2±0·3	3·8±0·4	11±5

Transcription assays were performed as described in Materials and Methods. Nucleotide and promoter concentrations were kept at saturating levels (400 μM ATP and CTP; 800 μM UTP; 200 nM template A).

† 1 mM GpG, for GpG-initiated pentamer.

‡ 4 mM GTP for GTP-initiated pentamer.

§ Values are taken from Table 5 which represent values obtained by varying one nucleotide concentration while keeping the other components at saturating levels (see Table 5 for details). These are averages of 2 to 4 experimental values.

synthesized the trimers substantially more efficiently than the pentamers on all three templates. The mutant Y639F showed comparable activity for the synthesis of the trimer GGA and the pentamer GGACU. The tetramers were synthesized to a much smaller extent than the trimers or the pentamers on template A and U, whereas on template C the synthesis of the tetramer was comparable to that of the pentamer. The relative production of trimers during tetramer and pentamer synthesis varied with the template. On template A, trimer products were much reduced under conditions permitting tetramer and pentamer synthesis, while on template U the

Table 9

Kinetic parameters for the synthesis of GpG-initiated and GTP-initiated trimer, tetramer and pentamer on template A by the wild-type enzyme

	$(K_m)_{app}$ (μM)			
Transcripts	ATP	CTP	UTP	$(k_{cat})_{app}$ (min^{-1})
GGA†	7±1			27±4 (15±2)
pppGGA†	5±3			48±4
GGAC†		3±1		3±1 (1·3±1)
pppGGAC†		7±1		14±7
GGACU†	19±2	6±1	138±78	7±2 (11±2)
pppGGACU‡	13±2	10±1	100±11	28±6 (19±2)

Transcription assays and calculations of $(K_m)_{app}$ and $(k_{cat})_{app}$ were made as described in Materials and Methods.

† Nucleotide and promoter concentrations were kept at saturating levels (400 μM GpG for GpG-initiated synthesis; 2 mM GTP for GTP-initiated synthesis; 400 μM ATP, CTP and UTP; 200 nM template A) except for varying nucleotide concentrations (5 to 100 μM ATP and CTP; 50 to 1000 μM UTP). Values in parentheses are obtained under saturating levels of nucleotides and promoter (1 mM GpG for GpG-initiated synthesis; 4 mM GTP for GTP-initiated synthesis; 400 μM ATP and CTP; 800 μM UTP; 200 nM template A).

‡ These are averages of 2 to 4 experimental values.

production of trimers was substantial during tetramer and pentamer synthesis. On template C, trimers and tetramers, as well as trimers and pentamers (plus possibly tetramers) were synthesized about equally, while tetramer synthesis increased relative to the other two templates. Thus, when the terminal nucleotide of the RNA synthesized is U, product synthesis is elevated. One explanation for this observation may be that the rate of RNA dissociation is higher for RNAs with terminal U. Our results also indicate that the rate of trimer dissociation becomes higher when the trimer is the end product relative to that observed when the tetramer is the end product. However, the rate of pentamer synthesis may be higher than that of the tetramer because the run-off product (pentamer) dissociates more rapidly. This interpretation of our data will be tested with further experiments.

Table 10
Kinetic parameters for the synthesis of trimers

Enzyme	Transcript	$(K_m)_{app}$ (μM)	$(k_{cat})_{app}$ (min^{-1})
		ATP	
WT	GpGp*A	7±2	27±4
Y639F		7±2	11±2
Y639S		73±13	0·3±0·1
H811A		250±50	3·2±1·7
		GTP	
WT	*pppGpGpA	220±30	8±2
Y639F		410±230	7±2

See Materials and Methods and Osumi-Davies *et al.* (1992) for reaction conditions and calculations of $(K_m)_{app}$ and $(k_{cat})_{app}$. For GGA synthesis, the GpG concentration was kept at 400 μM while the ATP concentration was varied from 5 to 100 μM for WT and Y639F, 25 to 200 μM for Y639S, and 50 to 800 μM for H811A. For pppGGA synthesis, the GTP concentration was varied from 100 μM to 2 mM and the ATP concentration was kept at 100 μM. Asterisks indicate the site of ^{32}P-labeling.

(g) *Steady-state kinetic parameters of the wild-type and the mutants Y639F, Y639S and synthesis of GGA by H811A on a 22 bp template*

Since it was not possible to obtain kinetic parameters for Y639S for the synthesis of pentamer, although this mutant exhibited a few percent of the activity of the wild-type enzyme, attempts were made to obtain the kinetic parameters for the synthesis of the trimers GGA and pppGGA in which a single nucleotide addition was examined. It was felt that this information might shed some light on the role of the phenyl ring of Tyr639. Reinitiation of trimer synthesis was examined to ensure that the enzyme was functioning catalytically and that product accumulation was linear within the measured time of the reaction. The kinetic parameters obtained for the synthesis of the trimers GGA and pppGGA by the Y639 mutants, along with values for the wild-type, are summarized in Table 10. For the incorporation of ATP in the presence of the initiating dinucleotide GpG, the mutant Y639S, which lacks the phenyl ring but retains the OH-group at position 639, showed a tenfold increase in $(K_m)_{app}$ and a ~100-fold decrease in $(k_{cat})_{app}$ compared to the values for the wild-type. Thus, the elimination of the phenyl ring appears to have a major impact on both $(K_m)_{app}$ and $(k_{cat})_{app}$. In contrast, the $(K_m)_{app}$ of Y639F remained the same as that of the wild-type, while $(k_{cat})_{app}$ was about a third of the value of the wild-type. The synthesis of pppGGA was introduced by employing [γ-^{32}P]GTP at varying concentrations of GTP. $(K_m)_{app}$ for GTP was twice as large as that of the wild-type but $(k_{cat})_{app}$ of Y639F remained unchanged. It was not possible to obtain reliable data for the synthesis of the trimer pppGGA which would permit determination of $(K_m)_{app}$ and $(k_{cat})_{app}$ for the mutant Y639S, but the data suggested that $(K_m)_{app}$ was very large.

The activity of the mutant H811A toward the synthesis of the trimer GGA was sufficient to permit kinetic parameters for the incorporation of ATP to be obtained (Table 10). A 35-fold increase in $(K_m)_{app}$ as well as a tenfold reduction in $(k_{cat})_{app}$ were observed, which indicates a major perturbation in nucleotide binding and the catalytic step for the addition of ATP to GpG.

(h) *pH-dependent enzyme activity for the wild-type and the mutants K631R and Y639F*

We also determined pH-dependent enzyme activities for the wild-type enzyme and the mutants K631R and Y639F. The observed apparent pK (~9·5) for the high-pH limb of the pH-activity profile of T7 RNA polymerase (Figure 7a) could be due to the titration of a perturbed lysine in the enzyme–substrate complex. The low-pH limb of the activity-pH profile is probably attributable to ionization of the nucleotides (Phillips *et al.*, 1963). If titration of Lys631 is responsible for the decline in T7 RNA polymerase activity at high pH, the $(pK)_{app}$ should be increased appreciably in K631R. In order to test this hypothesis, we have generated the mutant K631R for which activity for the synthesis of pppGGACU is about 13% that of wild-type on a 22 bp oligonucleotide template (template A). The high-pH limb of the activity data for the synthesis of pppGGACU was aligned with that of the 87 nt RNA synthesis shown in Figure 7a. In order to compare the pK values of the wild-type and mutant K631R more quantitatively, the pH-activity profiles on the high pH side were converted to $\log[(v/v_{max})/(1-(v/v_{max}))]$ which was plotted *versus* pH. As the results in Figure 7b show, the apparent pK values of the wild-type and mutant K631R are the same within experimental error, strongly suggesting that Lys631 is not the amino acid which titrates with the pK of ~9·5, and some other residue(s) govern the pH-activity profile. The mutant Y639F was also investigated and the apparent pK of this mutant was also comparable with that of the wild-type (Figure 7c), arguing that Tyr639 is not responsible for the pK at 9·5.

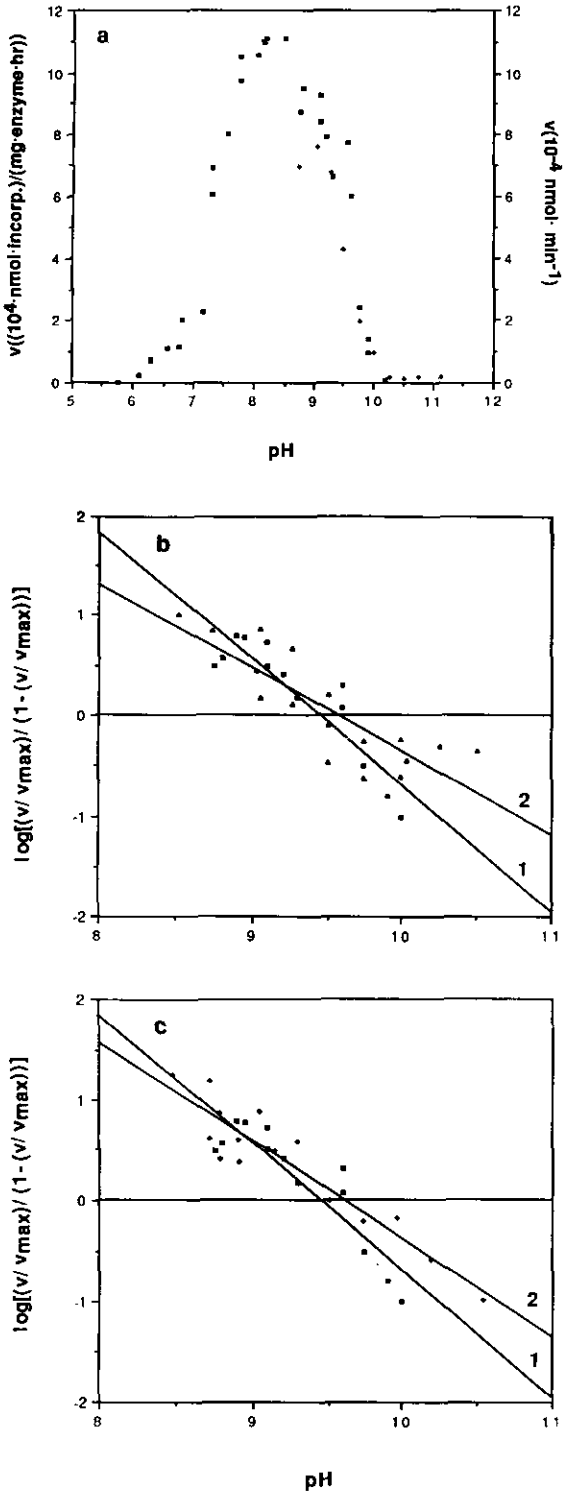

Figure 7. a, pH-activity profiles for the synthesis of 87 nt RNA and pppGGACU by the wild-type enzyme. Reactions were carried out (50 μl vol.) in 40 mM sodium phosphate (pH 5·5 to 7·25) or 40 mM Tris·HCl (pH 6 to 10) or 40 mM glycine-NaOH (pH 8·5 to 11·0), 10 mM $MgCl_2$, 1 mM DTT. Filled square: 87 nt RNA synthesized on 100 nM-*Hin*dIII-linearized pT713 plasmid, with 20 nM enzymes, 5 μCi [α-^{32}P]UTP, 2 mM GTP, and 800 μM UTP, ATP and CTP, at 37 °C for 5 min, and analyzed by a DE81 filter-binding method as described previously (Reisbig *et al.*, 1979). Cross: pentamer pppGGACU synthesized on template A (100 nM) under the same experimental conditions as described below (b). b and c, Plots of $\log[(v/v_{max})/(1-(v/v_{max}))]$ *versus* pH for the wild-type, the mutants K631R and Y639F. Reactions to synthesize the pentamer pppGGACU were carried out in the same buffers as in a with 100 nM template A, 20 nM enzyme, 2 mM GTP, 400 to 800 μM UTP, ATP, CTP, 5 μCi [^{3}H]UTP at 37 °C for 5 min, analyzed by urea/25% PAGE, and quantitated by PhosphorImager SP. Wild-type: filled square and line 1 in b; K631R: cross and line 2 in b. Wild-type filled square and line 1 in c; Y639F: filled triangle and line 2 in c.

4. Discussion

In this work, new mutations have been introduced at the five loci identified as essential (Asp537 and Asp812) and catalytically important (Lys631, Tyr639 and His811) in T7 RNA polymerase to generate enzyme molecules which have altered activities but remain catalytically competent, thus allowing further studies for comparison with the properties of the wild-type enzyme.

The results of CD measurements indicate that T7 RNA polymerase has a substantial amount of regular structure in solution (α, 43%; β, 14%; β-turn, 25%; unordered, 18%). The α-helix content of 43% is consistent with the characterization of T7 RNA polymerase as "highly helical" (Sousa *et al.*, 1993) and is similar to the helix content of 33 to 35% observed in the Klenow fragment from our analysis of the X-ray data (Ollis *et al.*, 1985). Our results differ markedly, however, from a previous report of 12% α-helix content for T7 RNA polymerase based on CD measurement (Oakley *et al.*, 1975). We have no explanation for this difference, but the spectrum we have obtained is substantially greater in amplitude than that of Oakley *et al.* (1975). With the exception of the mutant Y639W, which exhibits a somewhat lower α-helix content, the secondary structural data, T_m values determined by CD and DSC, and λ_{max} values from fluroescence spectra all indicate that the folding of these mutant T7 RNA polymerases is very similar to that of the wild-type. Therefore, the significant changes observed in the enzymatic activities of the mutants most probably reflect the functional involvement of the residues mutated, namely, D537, K631, Y639, H811 and D812.

These studies demonstrate that the negative charge or proton-accepting capability at amino acids Asp537 and Asp812 are essential for the activity of T7 RNA polymerase. Although the steady-state kinetic parameters are complex quantities and must be interpreted with caution, our kinetic results indicate that these Asp residues are involved in both nucleotide binding and subsequent chemical step(s). Work is in progress to elucidate possible roles of these two Asp residues in metal ion binding.

Additional proof that Lys631 participates in the stabilization of the transition state by co-ordinating the phosphoryl oxygen must come from another

source, such as detailed studies of individual kinetic steps using the mutant K631R. The amino acid responsible for the apparent pK_a (~9·5) obtained from the pH-activity profile was found not to be Lys631. The actual participating amino acid(s) has yet to be identified.

It also appears unlikely that the OH group of Tyr639 plays a significant role in T7 RNA polymerase catalysis since, when this residue is mutated to Phe, enzyme activity for the synthesis of the 5 nt RNA, pppGGACU, and 60 nt RNA is comparable to that of the wild-type (Osumi-Davis *et al.*, 1992; this work). This contradicts the proposal of Rechinsky *et al.* (1992) that the OH group of Tyr639 makes an H-bond to the 6-oxo group of G, because if this were the case the enzymatic activity of Y639F should be noticeably decreased relative to the wild-type enzyme.

Replacement of Tyr639 by Ser, which eliminates the phenyl ring but retains a hydroxyl group, produces a tenfold increase in $(K_m)_{app}$ for ATP and a ~50-fold reduction in $(k_{cat})_{app}$ for the synthesis of GGA. The phenyl ring could interact with the incoming nucleotides or align this substrate in a more catalytically efficient position, in contrast to the Ser residue. The corresponding tyrosine (Tyr766) in the Klenow fragment has been implicated in interaction with the incoming nucleotide based on chemical (Basu & Modak, 1987) and photoaffinity labeling (Rush & Konigsberg, 1990) studies.

This work also supports a catalytically significant role for His811 and suggests that one of its functions could be to enhance the nucleophilicity of a local Asp residue(s). That the mutant H811Q has 25% of the activity of the wild-type enzyme is consistent with this hypothesis. It is surprising, however, that the mutant H811A, which lacks H-bonding capability, is capable of synthesizing trimers and pentamers. Kinetic studies show that the mutation H811 to A811 increases $(K_m)_{app}$ by 35-fold and lowers $(k_{cat})_{app}$ by tenfold for the incorportion of ATP into GpG to form GGA on template A. While these are certainly major effects on nucleotide binding and phosphodiester bond formation, the observation of activity in H811A suggests that an H-bond from His811 may not be necessary. Alternatively, another side-chain might play a compensatory or complementary role in this mutant, or a water molecule might enter the space made available by the smaller Ala side-chain and contribute a functional H-bond, as has been seen in some other enzyme systems (Stayert *et al.*, 1990; Komives *et al.*, 1991; Kim *et al.*, 1992). If His811 functions as a structural anchor for another functional group, replacement of His by Ala could create a local perturbation in tertiary structure by misaligning a functionally important amino acid(s). If His811 interacts with an incoming nucleotide to properly align it for efficient catalysis, elimination of the His ring could drastically alter the alignment of the incoming nucleotide, thus resulting in a large increase in $(K_m)_{app}$ and a decrease in $(k_{cat})_{app}$.

Are there differences in the rate constants for the synthesis of GpG-initiated and GTP-initiated oligonucleotide synthesis? In the case of the wild-type and mutant Y639F enzymes, the apparent rate constants for the GpG-initiated pentamer synthesis are lower by approximately twofold than the values obtained for the GTP-initiated synthesis. In contrast, the two rate constants are comparable for the remaining viable mutants. However, there was approximately a twofold difference in the apparent rate constants for the same GTP-initiated pentamer synthesis depending upon the methods used to obtain these kinetic parameters (Table 8). We have also compared kinetic parameters for the GpG and GTP-initiated tri, tetra and penta-nucleotide synthesis by the wild-type enzyme (Table 9). In all cases, the $(k_{cat})_{app}$ values measured by varying the concentrations of nucleotides were greater than those obtained using "saturating levels" of all the nucleotides. There are two major problems with determining $(k_{cat})_{app}$ by velocity measurements at saturating substrate levels. First, it is difficult to be certain that all of the substrates are indeed at saturating levels, especially for initiating nucleotides. Second, high levels of one substrate can inhibit the incorporation of the others. Both of these effects will tend to produce lower values of $(k_{cat})_{app}$. With these problems in mind, the approximately twofold variation in some of the $(k_{cat})_{app}$ values may not be significant. Therefore, the presence of the 5′-triphosphate in the initiating nucleotide may have little effect on either the wild-type or the mutant T7 RNA polymerases. Martin & Coleman (1989) showed that substitution of GTP with guanosine or GMP had little effect on the synthesis of tetramer GACU. A more refined kinetic method will be necessary to address this question more precisely.

The third nucleotide on template U is UTP and the fourth nucleotide on template C is UTP. Our data imply that RNA dissociation is faster in the presence of terminal U, and premature termination occurs more frequently after UMP incorporation. This is true not only for the wild-type enzyme but also for all the viable mutants we have examined (Table 7). The relatively weak dA·rU base-pair (Martin & Tinoco, 1980) may explain this observation. Premature termination occurring immediately after UMP incorporation during the synthesis of oligonucleotides was also observed by Martin *et al.* (1988) with the wild-type T7 RNA polymerase.

Three possible types of rate-determining steps can be considered in the mechanism of RNA polymerases: (1) formation of the first phosphodiester bond, i.e. addition of the first nucleotide to GTP or GpG initiator; (2) subsequent incorporation of nucleotides into the growing chain; and (3) dissociation of the product. All three types could include associated enzyme conformational changes. The wild-type and mutant T7 RNA polymerases may have different rate-determining steps. In the wild-type enzyme, it is likely that the rate-determining step is either (1) or (3) for short oligonucleotides. Except for Y639F, the $(k_{cat})_{app}$ value for GTP-initiated pentanucleotide

synthesis is decreased for all mutants, and the mutant enzymes exhibit a higher ratio of abortive products to longer transcripts. These results may be attributed to a reduced rate for the subsequent nucleotide addition step which becomes rate-limiting in the mutants. In the case of the Y639F, $(k_{cat})_{app}$ appears to increase, but only slightly. This implies that the Y639F mutation has only a minor effect on the rate of the subsequent nucleotide addition step and therefore dissociation and/or initial phosphodiester bond formation remain rate-limiting.

Bonner *et al.* (1992) have investigated some of the same mutants described here (D537E, Y639F, Y639S, Y639A, H811A, D812N, D812E). Although they did not investigate the kinetics of RNA synthesis in as much detail as presented here, they did report K_m and V_{max} values for transcription of a supercoiled plasmid carrying a T7 promoter. The different nature of the templates used in our studies precludes direct comparison of absolute values of k_{cat} and K_m values, but relative values should be comparable. All of the mutants which we have also studied were reported by Bonner *et al.* to show less than a twofold variation in K_m, whereas we have observed three- to fourfold variations in K_m for GTP and UTP between wild-type and D812E enzymes. The wider range in K_m observed in this study may result from producing an RNA in which each NTP is incorporated at a single site (except for GTP). By contrast, Bonner *et al.* measured the K_m values for incorporation in all possible sequence contexts and this may have evened out differences among the mutants. The relative values of V_{max} reported by Bonner *et al.* (1992), however, differ strikingly from the values we have obtained. Whereas Bonner *et al.* find an approximately 30-fold reduction in V_{max} for D537E relative to wild-type, we find (Tables 5 and 6) only 1·4-fold, 4-fold and 1·5-fold reductions in $(k_{cat})_{app}$ values for pppGGACU and GGACU and GGA synthesis, respectively. For D813E, a 300-fold reduction in V_{max} was reported by Bonner *et al.*, while in our system, there are about twofold and fivefold reductions in $(k_{cat})_{app}$ values for pppGGACU and GGACU, respectively, and a small increase for GGA. It should be noted that Bonner *et al.* studied nucleotide incorporation dominated by elongation complexes, while our results are confined to initiation complexes. The large differences in our results may imply that the kinetics are very different in the two types of complex, and that some mutations most strongly affect k_{cat} in the elongation complex (D537E, H811A, D812E), while others (Y639F) primarily alter k_{cat} in the initiation complex. It may also be that in the synthesis of a long RNA, premature termination or pausing as a result of an increased K_m or decreased k_{cat} value cause a larger reduction in V_{max} for the synthesis of a long RNA.

Through this study, we have obtained new information to support our earlier observations concerning the five catalytically important amino acids identified in the active site of T7 RNA polymerase through photoaffinity labeling studies (Knoll *et al.*, 1992) and site-directed mutagenesis (Osumi-Davis *et al.*, 1992), and have gained insight into some of their possible functional roles. Our hypothesis that these amino acid residues lie in the active site in a manner similar to the homologous residues in *Escherichia coli* DNA polymerase I has been supported by the subsequent work of Bonner *et al.* (1992) and by the recent X-ray structure of T7 RNA polymerase at 3·3 Å resolution (Sousa *et al.*, 1993). T7 RNA polymerase shows extensive structural homology to the polymerase domain of Klenow fragment, and the fully conserved D537, K631, Y639, G640, D812, and the less fully conserved H811 are all present in the putative catalytic site.

Much work is needed before we can understand how all these functional groups, and functional groups yet to be recognized, work together to bring about catalysis. Although much can be learnt about related enzymes through homology alignment, RNA polymerase has a unique specificity, which needs to be explored through specific experiments on each particular RNA polymerase. The Klenow fragment has three carboxylate groups, Asp705, Asp882 and Glu883, which are thought to be critical for DNA polymerase I activity (Steitz, 1993). By contrast, T7 RNA polymerase has neither an Asp nor a Glu immediately downstream from Asp812, the homolog of Asp882 in the Klenow fragment (Delarue *et al.*, 1990). In addition, the substrate requirements are different for the two enzymes, emphasizing that although the conserved amino acids throughout the polymerase group are important, amino acids yet to be identified could be central to the unique specificity of the two classes of polymerases.

The authors acknowledge the technical assistance of A. M. Verticelli and K. E. Marfia with the fluorescence and calorimetry experiments. This research was supported by U.S. Public Health Service grant GM-23697.

References

Basu, A. & Modak, M. J. (1987). Identification and amino acid sequence of the deoxynucleoside triphosphate binding site in *Escherichia coli* DNA polymerase I. *Biochemistry*, **26**, 1704–1709.

Bonner, G., Patra, D., Lafer, E. M. & Sousa, R. (1992). Mutations in T7 RNA polymerase that support the proposal for a common polymerase active site structure. *EMBO J.* **11**, 3767–3775.

Davanloo, P., Rosenberg, A. H., Dunn, J. J. & Studier, F. W. (1984). Cloning and expression of the gene for bacteriophage T7 RNA polymerase. *Proc. Nat. Acad. Sci., U.S.A.* **81**, 2035–2039.

Delarue, M., Poch, O., Tordo, N., Moras, D. & Argos, P. (1990). An attempt to unify the structure of polymerases. *Protein Eng.* **3**, 461–467.

Kabsch, W. & Sander, S. (1983). Dictionary of protein secondary structures: pattern recognition of H-bonded and geometric features. *Biopolymers*, **22**, 2579–2637.

Kim, Y., Mlsna, D., Monzingo, A. F., Ready, M. P., Frankel, A. & Robertus, J. D. (1992). Structure of

ricin mutant showing rescue to activity by a non-catalytic residue. *Biochemistry*, **31**, 3294–3296.

King, G. C., Martin, C. T., Pham, T. T. & Coleman, J. E. (1986). Transcription by T7 RNA polymerase is not zinc-dependent and is abolished on amidomethylation of cysteine-347. *Biochemistry*, **25**, 36–40.

Komives, E. A., Chang, L. E., Lolis, E., Tilton, R. F., Petsko, G. A. & Knowles, J. R. (1991). Electrophilic catalysis in triosephosphate isomerase: the role of histidine-95. *Biochemistry*, **30**, 3011–3019.

Knoll, D. A., Woody, R. W. & Woody, A-Y. M. (1992). Mapping of the active site of T7 RNA polymerase with 8-azidoATP. *Biochim. Biophys. Acta*, **1121**, 252–260.

Martin, C. T. & Coleman, J. E. (1987). Kinetic analysis of T7 RNA polymerase-promoter interactions with small synthetic promoters. *Biochemistry*, **27**, 2690–2696.

Martin, C. T. & Coleman, J. E. (1989). T7 RNA polymerase does not interact with the 5′-phosphate of the initiating nucleotide. *Biochemistry*, **28**, 2760–2762.

Martin, C. T., Muller, D. K. & Coleman, J. E. (1988). Processivity in early stages of transcription by T7 RNA polymerase. *Biochemistry*, **27**, 3966–3974.

Martin, F. H. & Tinoco, I. (1980). DNA–RNA hybrid duplexes containing oligo(dA : rU) sequences are exceptionally unstable and may facilitate termination of transcription. *Nucl. Acids Res.* **8**, 2295–2299.

Moffatt, B. A., Dunn, J. J. & Studier, F. W. (1984). Nucleotide sequence of the gene for bacteriophage T7 RNA polymerase. *J. Mol. Biol.* **173**, 265–269.

Oakley, J. H., Pascale, J. A. & Coleman, J. E. (1975). T7 RNA polymerase: conformation, functional groups, and promoter binding. *Biochemistry*, **14**, 4684–4691.

Ollis, D. L., Brick, P., Hamlin, R., Xuong, N. G. & Steitz, T. A. (1985). Structure of large fragment of *Escherichia coli* DNA polymerase I complexed with dTMP. *Nature (London)*, **313**, 762–766.

Osumi-Davis, P. A., de Aguillera, M. C., Woody, R. W. & Woody, A-Y. M. (1992). Asp537, Asp812 are essential and Lys631, His811 are catalytically significant in bacteriophage T7 RNA polymerase activity. *J. Mol. Biol.* **226**, 37–45.

Phillips, R. C., George, P. & Rutman, R. J. (1963). Potentiometric studies of the secondary phosphate ionizations of AMP, ADP and ATP, and calculations of thermodynamic data for the hydrolysis reaction. *Biochemistry*, **2**, 501–508.

Press, W. H., Flannery, B. P., Teukolsky, S. A. & Vetterlin, W. T. (1989). *Numerical Recipes. The Art of Scientific Computing* (FORTRAN version), pp. 523–528, Cambridge University Press, Cambridge, U.K.

Rechinsky, V. O., Kostyuk, D. A., Tunitskaya, V. L. & Kochetkov, S. N. (1992). On the functional role of the Tyr639 residue of bacteriophage T7 RNA polymerase. *FEBS Letters*, **306**, 129–132.

Reisbig, R. R., Woody, A-Y. M. & Woody, R. W. (1979). Spectroscopic analysis of the interaction of *Escherichia coli* DNA-dependent RNA polymerase with T7 DNA and synthetic polynucleotides. *J. Biol. Chem.* **254**, 11208–11217.

Rush, J. & Konigsberg, W. H. (1990). Photoaffinity labeling of the Klenow Fragment with 8-Azido-dATP. *J. Biol. Chem.* **265**, 4821–4827.

Sousa, R., Chung, Y. J., Rose, J. P. & Wang, B. C. (1993). Crystal structure of bacteriophage T7 RNA polymerase at 3·3 Å resolution. *Nature (London)*, **364**, 593–599.

Sreerama, N. & Woody, R. W. (1993). A self consistent method for the analysis of protein secondary structure from circular dichroism. *Anal. Biochem.* **209**, 32–44.

Stayert, J., Hallenga, K., Wyns, L. & Stassen, P. (1990). Histidine-40 of ribonuclease T_1 acts as a base catalyst when the true catalytic base, glutamic acid-58, is replaced by alanine. *Biochemistry*, **29**, 9064–9072.

Steadman, B. L., Trautman, P. A., Lawson, E. Q., Raymond, M. J., Mood, D. A., Thomson, J. A. & Middaugh, C. R. (1989). A differential scanning study of the bovine lens crystallins. *Biochemistry*, **28**, 9653–9658.

Steitz, T. A. (1993). DNA- and RNA-dependent DNA polymerases. *Curr. Opin. Struct. Biol.* **3**, 31–38.

Tabor, S. & Richardson, C. C. (1985). A bacteriophage T7 RNA polymerase/promoter system for controlled exclusive expression of specific genes. *Proc. Nat. Acad. Sci., U.S.A.* **82**, 1074–1078.

Wilkinson, G. N. (1961). Statistical estimation in enzyme kinetics. *Biochem. J.* **80**, 324–332.

Edited by D. Draper

(Received 19 May 1993; accepted 30 November 1993)